

1 © 2019. This is the pre-print (submitted) version of the following article: “K. Wagner, G.  
2 Häggström, A.M. Mauerhofer, M. Kuba, N. Skoglund, M. Öhman, H. Hofbauer, Layer  
3 formation on K-feldspar in fluidized bed combustion and gasification of bark and chicken  
4 manure, Biomass and Bioenergy. 127 (2019) 105251.  
5 <https://doi.org/10.1016/j.biombioe.2019.05.020>.”, which has been published in final form at  
6 <https://doi.org/10.1016/j.biombioe.2019.05.020>. This pre-print version is made available  
7 under the CC-BY-NC-ND 4.0 license <http://creativecommons.org/licenses/by-nc-nd/4.0/>.

# 8 Layer Formation on K-feldspar in 9 Fluidized Bed Combustion and 10 Gasification with bark and chicken 11 manure

---

12 Katharina Wagner<sup>a,b,\*</sup>, Gustav Häggström<sup>c</sup>, Anna Magdalena Mauerhofer<sup>b</sup>, Matthias  
13 Kuba<sup>a,b,c,d,\*</sup>, Nils Skoglund<sup>d</sup>, Marcus Öhman<sup>c</sup>, Hermann Hofbauer<sup>b</sup>

14 <sup>a</sup>Bioenergy 2020+ GmbH, Wienerstraße 49, A-7540 Güssing, Austria

15 <sup>b</sup>Institute of Chemical, Environmental & Bioscience Engineering, TU Wien, Getreidemarkt  
16 9/166, A-1060 Vienna, Austria

17 <sup>c</sup>Energy Engineering, Division of Energy Science, Luleå University of Technology, SE-971 87  
18 Luleå, Sweden

19 <sup>d</sup>Thermochemical Energy Conversion Laboratory, Department of Applied Physics and  
20 Electronics, Umeå University, SE-901 87 Umeå, Sweden

21 \*Corresponding author: [matthias.kuba@bioenergy2020.eu](mailto:matthias.kuba@bioenergy2020.eu)

22 T: +43 3322 42606-156

23 F: + 43 3322 42606-199

24

25 [katharina.wagner@bioenergy2020.eu](mailto:katharina.wagner@bioenergy2020.eu)

26 T: +43 (3322) 42606-165

27 F: + 43 3322 42606-199

28

## 29 **Abstract**

30 The layer formation on bed materials in fluidized bed applications is an often-studied  
31 phenomenon where most work has focused on combustion but some studies on gasification  
32 exists, and direct comparisons of layer formation in combustion and gasification have been

33 performed occasionally. The present work provides a thorough comparison of layer formation  
 34 during combustion and gasification with K-feldspar as bed material using different  
 35 feedstocks, namely Ca-rich bark; Ca- and P-rich chicken manure; and an admixture of  
 36 chicken manure with bark. The feedstocks are tested in a 5 kW bubbling fluidized bed  
 37 combustor and a 100 kW<sub>th</sub> dual fluidized bed steam gasifier. A reference bed material sample  
 38 from the industrial biomass combined heat and power plant (CHP) in Senden is used as  
 39 example for the gasification of bark-rich logging residues. The formed bed particle layers on  
 40 the bed material surface are characterised using combined scanning electron microscopy  
 41 and energy-dispersive X-ray spectroscopy; area mappings and line scans are carried out for  
 42 all samples. The obtained data shows no essential influence of operational mode on the  
 43 layer formation process. During the combustion and gasification of Ca-rich feedstocks a layer  
 44 rich in Ca formed while K is diffusing out of the layer. The use of Ca- and P-rich feedstocks  
 45 inhibited the diffusion of K and a layer rich in Ca and also P formed. The addition of P to the  
 46 feedstock by chicken manure therefore changed the underlying layer formation processes.

## 47 **Keywords**

48 Fluidized bed, layer formation, K-feldspar, P, combustion, gasification

## 49 **Highlights**

- 50 • Layer formation on K-feldspar is the same during combustion and gasification
- 51 • P-rich chicken manure promotes the formation of phosphates in layers
- 52 • P-rich chicken manure hinders diffusion of K out of the K-feldspar particles

## 53 **1. Introduction**

54 The Holocene epoch, which already lasts for more than 11,700 years, is the only state of the  
 55 earth system to be known of supporting contemporary human societies. Human activities  
 56 since the age of industrialization are strongly influencing the earth system increasing the risk  
 57 of destabilization, resulting in a state less hospitable to the development of human societies.  
 58 Nine planetary boundaries that define a safe operating space for human societies have been  
 59 defined, as displayed in Figure 1. [1]

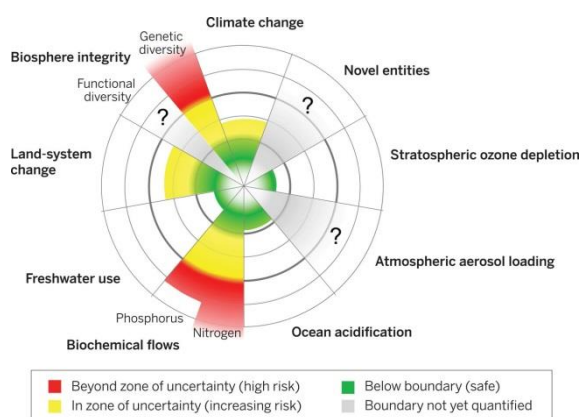


**Figure 1. Current status of seven of nine planetary boundaries [1].**

60 The biogeochemical flow of P is one of the planetary boundaries already in a high risk zone.  
 61 Addressing the further use and possible recovery potential of waste streams containing

62 relevant amounts of P is therefore of major importance. The use of such P-rich waste  
63 streams as feedstock in thermochemical conversion applications (e.g. combustion,  
64 gasification) is one strategy to address the challenge with biogeochemical flows of P by both  
65 reducing waste and enabling recovery and recycling.

66 Fluidized bed technology is a promising application for such thermochemical conversion of  
67 biogenic feedstock. Thermal conversion in fluidized beds allows for utilization of different  
68 feedstock [2] and is an industrial established technology. Thermochemical gasification of  
69 biogenic feedstock is a promising option to advance the eco-friendly and efficient production  
70 of secondary energy carriers, heat and power generation out of the product gas. The dual  
71 fluidized bed (DFB) steam gasification of bark-rich logging residues demonstrates a well-  
72 proven technology to produce nitrogen-free product gas with a heating value of around  
73 11-15 MJ Nm<sup>-3</sup>. The basic principle of the process is shown in Figure 2. This process is  
74 based on the separation of endothermic gasification and exothermic combustion. Heat, which  
75 is necessary for gasification, is provided by the circulating bed material from the combustion  
76 to the gasification reactor. Steam is used as gasification agent for the bubbling bed in the  
77 gasification reactor. A part of the biomass is combusted to provide the heat necessary for  
78 gasification [3]. A comprehensive review on the DFB gasification technology was recently  
79 published by Karl and Pröll [4].

80 Based on this concept the first industrial application using wood as feedstock was  
81 commissioned in the early 2000's with the combined heat and power plant Güssing in Austria  
82 (8 MW<sub>th</sub> feedstock capacity). Further plants went into operation in Oberwart/Austria (9 MW  
83 fuel capacity), Villach/Austria (15 MW<sub>th</sub> feedstock capacity), Senden/Germany (14 MW<sub>th</sub>  
84 feedstock capacity), and in Göteborg/Sweden (32 MW<sub>th</sub> feedstock capacity).

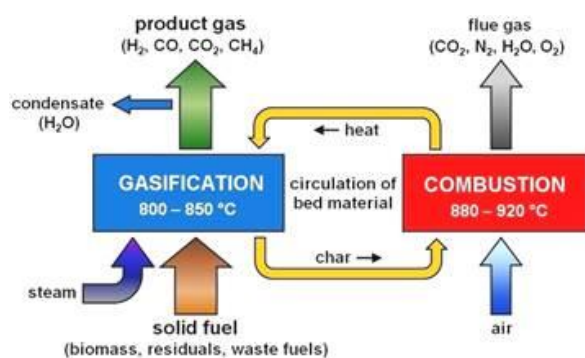


**Figure 2. Basic principle of DFB steam gasification [3].**

85 The economic feasibility of biomass projects is highly dependent on the feedstock price.  
86 Additionally, biogenic feedstock should not be in competition with food production. To reduce  
87 feedstock costs biogenic residues are a promising alternative to woody biomass. One of the  
88 challenging issues for the utilization of residues for gasification is the high ash content, which  
89 contains various elements. Understanding the ash chemistry in the system is a key factor for  
90 further development of the technology [5].

91 Interactions between feedstock ash and bed material particles have been investigated in the  
92 past. Ash layer formation has been described on a mechanistic level for combustion of  
93 various feedstocks and for gasification of bark-rich logging residues [2,6-8]. Furthermore,  
94 positive catalytic effects have been assigned to Ca-rich ash layers in gasification leading to  
95 an improvement of the product gas quality compared to fresh olivine [9,10]. A kinetic rate  
96 expression was empirically derived for olivine after an ash-rich layer has formed [11].

97 Berdugo Vilches et al. proposed a first overview of the main transformation reactions  
98 pathways of tar species when olivine, activated through interaction with ash components, is  
99 used as in-bed catalyst [12]. Optimization of the operation of an industrial-scale DFB steam  
100 gasification plant based on the activation of the bed material through interaction with  
101 feedstock ash was reported by Kuba et al. [13]. Here, already catalytically activated olivine  
102 bed particles were reused in the process to increase the overall activity of the fluidized bed.  
103 Similar results regarding the optimization in industrial-scale were obtained at the DFB steam  
104 gasifier GoBiGas, where ash components were identified to play a major role in improving  
105 the product gas quality [14].

106 First insights into ash layer formation in both combustion and gasification [15,16] have been  
107 reported, indicating that the operational mode has no influence on the layer formation, apart  
108 from S-rich feedstocks, where the formation of a melt only occurring during combustion  
109 enhances the agglomeration tendency of S-rich feedstocks [15]. The influence of P on the  
110 layer formation has been studied in combustion [2] and gasification [17] atmosphere, but to  
111 the authors' knowledge no study focused on a comparison of P-rich feedstocks in both  
112 combustion and gasification atmosphere. Several groups currently focus on the substitution  
113 of olivine as bed material in DFB steam gasification [17–26] due to its heavy metal content  
114 [8]. K-feldspar was found as impurity in CHP in Senden, where layers rich in Ca developed  
115 and thermochemical analysis showed that these layers show a lower tendency towards  
116 agglomeration compared to layers formed on quartz particles [8]. Alkali-feldspar (a mixture of  
117 K-feldspar and Na-feldspar, with traces of Ca-feldspar) was shown to have a catalytic activity  
118 towards tar reforming [19] and was tested as bed material in the Chalmers 2-MW gasifier  
119 [18]. No catalytic activity towards the water-gas-shift reaction was detected for pure K-  
120 feldspar [17,27] but it was possible to activate the K-feldspar by layer formation during the  
121 gasification in a 100 kW<sub>th</sub> DFB reactor at TU Wien with a mixture of bark, straw, and chicken  
122 manure as feedstock [17].

123 Therefore, this paper addresses the influence of P on the layer formation both in fluidized  
124 bed combustion and gasification with K-feldspar as bed material. Samples from both fluidized  
125 bed combustion as well as DFB steam gasification facilities were evaluated. Furthermore, the  
126 influence of P from the feedstock regarding layer formation is addressed. For this, P-lean  
127 bark, P-rich chicken manure, and an admixture of chicken manure to bark are compared  
128 regarding their layer formation process.

## 129 **2. Materials and Methods**

130

131 Bed material samples were collected from fluidized bed combustion as well as gasification  
132 and compared regarding their layer formation. The combustion experiments were carried out  
133 in a 5 kW bubbling fluidized bed reactor. Bed material samples for gasification were obtained  
134 from the CHP (15 MW<sub>th</sub>) in Senden and from a 100 kW<sub>th</sub> DFB pilot plant at TU Wien.

### 135 **2.1. Feedstocks**

136 The feedstocks used for these investigations were conifer bark during combustion and bark-  
137 rich logging residues for gasification; a mixture of bark with chicken manure (ratio 7:3 dry  
138 mass) during combustion and gasification; and pure chicken manure during combustion and  
139 gasification. Table 1 shows relevant data for the feedstocks used. The ash content was

140 determined according to DIN 14775 but at a temperature of 550 °C and the lower heating  
 141 value was determined according to DIN 51900 T2.

142 **Table 1. Ash content and LHV of the used feedstocks. The table also gives an overview of the reactors**  
 143 **that each feedstock was used in.**

Fuel	Used in	Ash content mass fraction given in % d.b. <sup>a</sup>	LHV <sup>b</sup> kJ kg <sup>-1</sup> (d.b. <sup>a</sup> )
Bark	5 kW <sub>th</sub> BFB Combustion	8.1	18180
Bark-rich logging residues	15 MW <sub>th</sub> CHP Senden	1.5	17920
Bark+chicken manure (7:3)	5 kW <sub>th</sub> BFB Combustion + 100 kW <sub>th</sub> DFB	13.5	16430
Chicken manure	5 kW <sub>th</sub> BFB Combustion+ 100 kW <sub>th</sub> DFB	25.4	13900

144 <sup>a</sup> dry basis, <sup>b</sup> lower heating value

145 Figure 3 shows the feedstock ash components (fuel fingerprint) of the used feedstocks,  
 146 determined using XRF. Displaying the ash composition in mol kg<sup>-1</sup> gives a better overview of  
 147 the possible interactions taking place in the ash [28]. The used values to obtain Figure 3 are  
 148 given in the supplementary in Table .

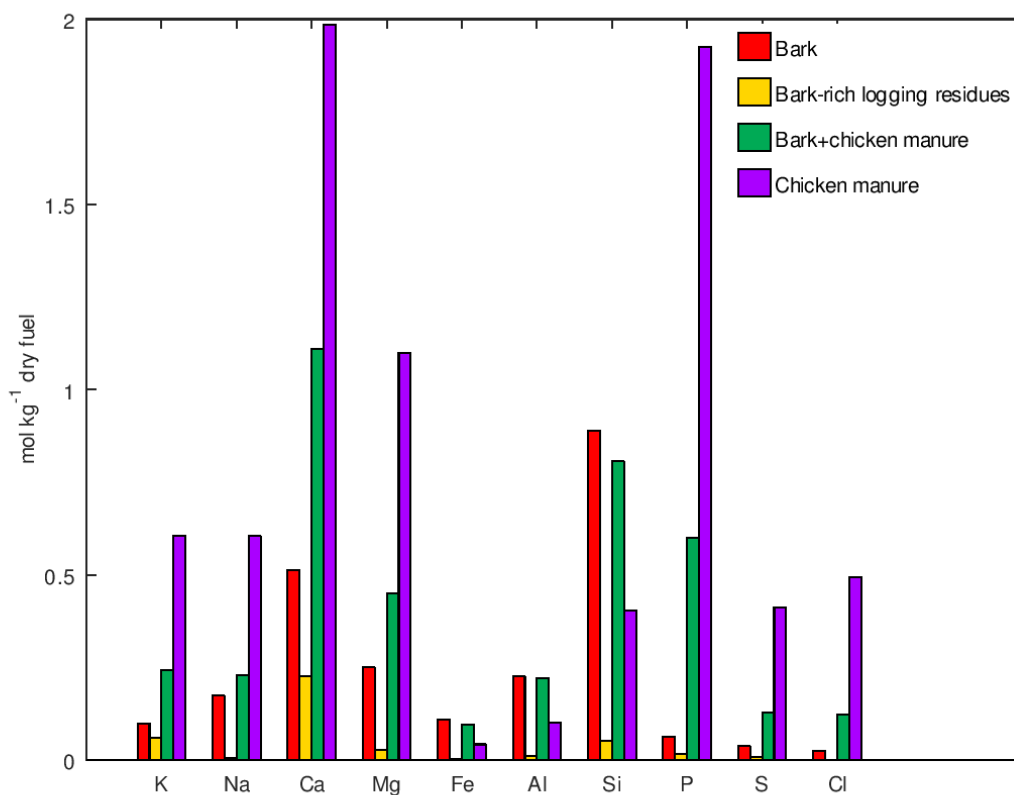


**Figure 3. Feedstock ash components in the used feedstocks.**

## 2.2. Bed material

Feldspar is currently investigated comprehensively as bed material for DFB steam gasification [17–19]. K-feldspar has a mohs' hardness of 6 and its density is  $2600 \text{ kg m}^{-3}$ . Additionally, it is an easily available mineral and therefore a promising bed material especially for gasification.

For the combustion experiments in the 5 kW test rig, K-feldspar was sieved to a particle size of 200 - 250  $\mu\text{m}$  as needed for the bubbling fluidized bed reactor. The K-feldspar studied from the CHP in Senden is an "impurity" introduced with the feedstock into the olivine bed, which is currently used in commercial DFB gasifiers. For the gasification test campaigns in the 100 kW DFB pilot plant a mixture of  $0.89 \text{ kg kg}^{-1}$  K-feldspar ( $d_{\text{SV}} = 287 \mu\text{m}$ ) and  $0.11 \text{ kg kg}^{-1}$  limestone ( $d_{\text{SV}}=480 \mu\text{m}$ ) was used. The calcite was added to increase the catalytic activity of the bed during start-up, since the pure and unused K-feldspar does not possess any catalytic activity [17,27].

## 2.3. Fluidized bed reactors for experimental investigations

Combustion experiments were conducted in a 5 kW bubbling fluidized bed (BFB) reactor. The total height of the reactor is 2 m with an inner diameter of 100 mm at the air distribution plate and 200 mm in the freeboard section. Temperatures and pressures could be monitored continuously. The fluidized bed was maintained with a primary air flow of  $50 \text{ NL min}^{-1}$  through the distribution plate below the bed. The primary air velocity was approximately six times the minimum fluidization velocity which translates to about  $0.6 \text{ m s}^{-1}$ . A secondary air flow of  $30 \text{ NL min}^{-1}$  was introduced into the reactor above the fluidized bed into the freeboard providing sufficient oxygen to ensure complete combustion of the generated gases. The reactor was equipped with external heaters for heat up and compensation of heat losses. The temperature inside the reactor is regulated by these heaters as well as by the feedstock input. The flue gas is cleaned by a cyclone removing all particles larger than  $10 \mu\text{m}$ . Afterwards the flue gas is further cleaned with a water scrubber. A more detailed description can be found elsewhere [29]. In total, 540 g of the sieved bed material were added to the fluidized bed. The operating temperature during the combustion experiments were around  $800 \text{ }^\circ\text{C}$  and feedstock was continuously fed with a rate around  $0.7 \text{ kg h}^{-1}$  for 40 hours or until the bed collapsed due to agglomeration of the bed material. Bed material samples were taken after the experiments and were then further analysed regarding layer formation.

The bed material sample for the gasification of bark-rich logging residues was taken from the CHP in Senden. The studied K-feldspar particles are "impurities" introduced by the feedstock. The data presented in this work is also described in an earlier work [8].

Gasification experiments with bark+chicken manure and chicken manure were conducted in a  $100 \text{ kW}_{\text{th}}$  DFB pilot plant at TU Wien. A detailed description on the specific design of the reactor system can be found in literature [30]. For the gasification test campaigns the DFB steam gasifier was first heated up with electrical trace heating and later on additionally by combusting softwood pellets until the desired temperatures were reached. At that point steam fluidization was started in the gasification reactor until a steady-state operation was achieved. During this gasification test campaigns several feedstocks were tested. At first, a benchmark operation with softwood pellets was carried out, further described elsewhere [20]. Afterwards the test campaign with bark+chicken manure pellets was started, before ending with the chicken manure pellets only. Bed material samples were taken before each fuel

194 change from the lower loop seal.

195 Table 2 summarizes the experiments covered in this work. It gives an overview of the  
196 average temperatures observed and the operation time when the samples were taken. For  
197 the combustion experiments  $T_{\text{combustion}}$  describes the temperature in the fluidized bed, while  
198 for the gasification experiments  $T_{\text{combustion}}$  describes the temperatures measured in the  
199 combustion reactor and  $T_{\text{gasification}}$  the temperatures in the gasification reactor. The  
200 operational times of the compared experiments differ greatly, as can be seen in Table 2. At  
201 this point it is worth mentioning that the combustion experiment with chicken manure did not  
202 lead to defluidization but was stopped intentionally due to the accumulating ash inside the  
203 system.

204 **Table 2. Average temperatures measured during the operation and duration of operation when the sample**  
205 **was taken.**

		Combustion (5 kW)			Gasification		
		Bark	Bark+ chicken manure	Chicken manure	Bark-rich logging residues (15 MW) [8]	Bark+ chicken manure (100 kW)	Chicken manure (100 kW)
$T_{\text{combustion}}$	°C	826	795	804	884	996	952
$T_{\text{gasification}}$	°C	n.a. <sup>a</sup>	n.a. <sup>a</sup>	n.a. <sup>a</sup>	856	777	766
$t_{\text{operation}}$	h	36.5	40	10.8	Constant bed replacement	2.9	1.9

206 <sup>a</sup> not applicable

## 207 **2.4. Scanning electron microscopy with energy dispersive** 208 **spectroscopy**

209 For all analyses, the materials were mounted in epoxy and polished to obtain cross sections  
210 of bed particles. Combined scanning electron microscope (SEM) and energy-dispersive X-  
211 ray spectroscopy (EDS) area mappings and line scans were applied to study the bed  
212 materials. Layer morphology in the samples was determined with a Zeiss Evo LS-15 at a  
213 voltage of 20 kV and a current of 400 pA in backscattered mode; elemental composition was  
214 determined using an Oxford X-MaxN 80 EDS detector. Overview images were captured to  
215 identify typical bed particles for elemental analysis. In each sample, around 30 line scans  
216 distributed over several particles and approximately five area mappings were obtained.

## 217 **3. Results and Discussion**

218

219 Table 3 depicts SEM images and EDS measurements obtained for the samples of the  
220 experiments. The SEM images show, that an observable layer formed for all experiments.  
221 The EDS measurements show, that during all experiments layers rich in Ca were formed. P  
222 was only found in the layers if a P-rich feedstock was used. During the combustion  
223 experiments with bark+chicken manure and chicken manure S was non-continuously  
224 detected in layers as well. The observed composition of these S-containing areas  
225 corresponds to analyses done for ash particles found in the bed, which will be the focus of an  
226 upcoming work.

227 Figure 4 shows a close-up of a K-feldspar particle obtained from the combustion of  
228 bark+chicken manure and Table 4 shows corresponding EDS images. A clear layer

229 formation can be observed in the micrograph. The cracks in the layer probably stem from the  
 230 preparation of the sample since no differences in elemental composition along the cracks are  
 231 observable in the EDS images. The EDS images clearly show that Ca is found further into  
 232 the particle compared to Mg and phosphorous.

233 **Table 3. SEM and EDS analysis of K-feldspar particles for the experiments with bark, bark+chicken**  
 234 **manure, and chicken manure in combustion and gasification atmosphere.**

	Combustion			Gasification		
	Bark	Bark+chicken manure	Chicken manure	Bark	Bark+chicken manure	Chicken manure
SEM-Image						
K						
Na						
Ca						
Mg						
Al						
Si						
P						
S						

235



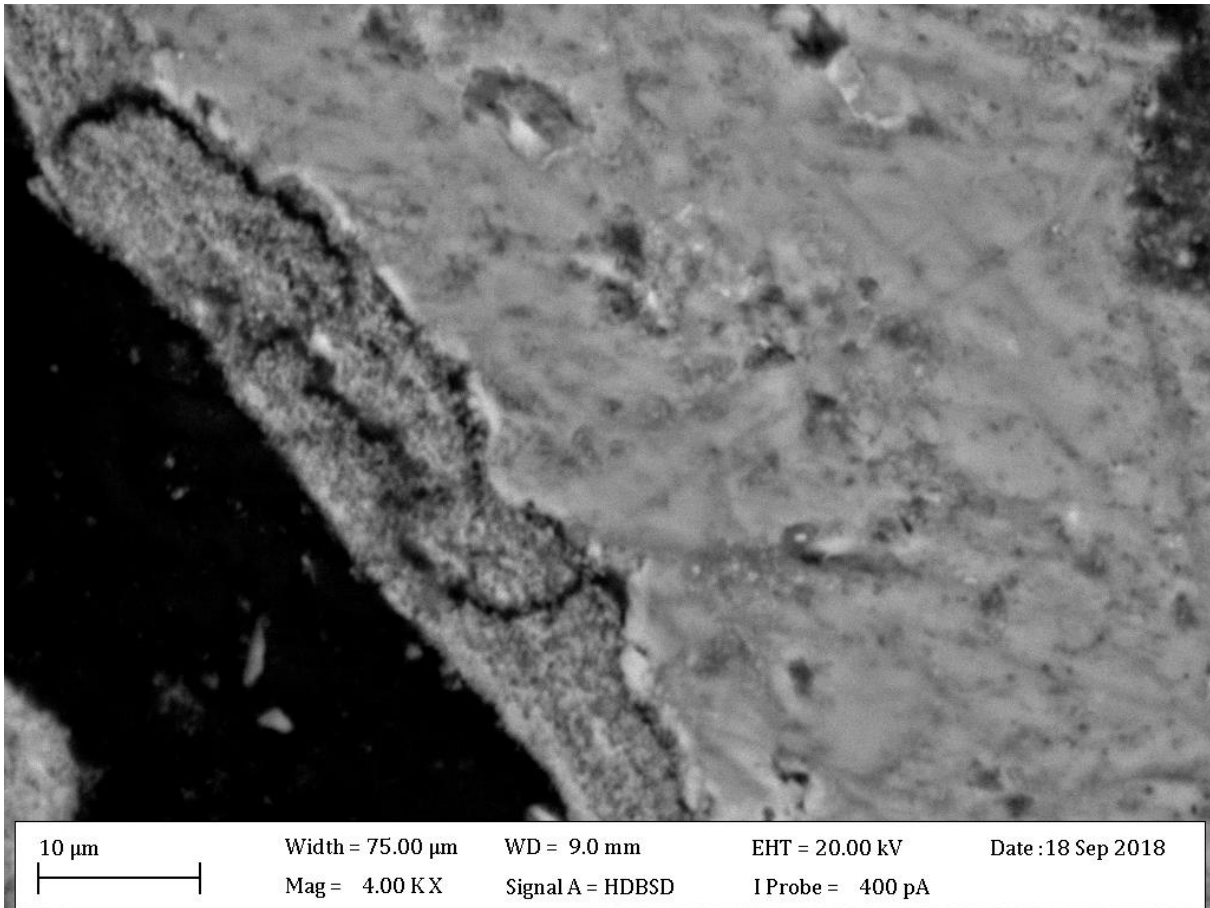
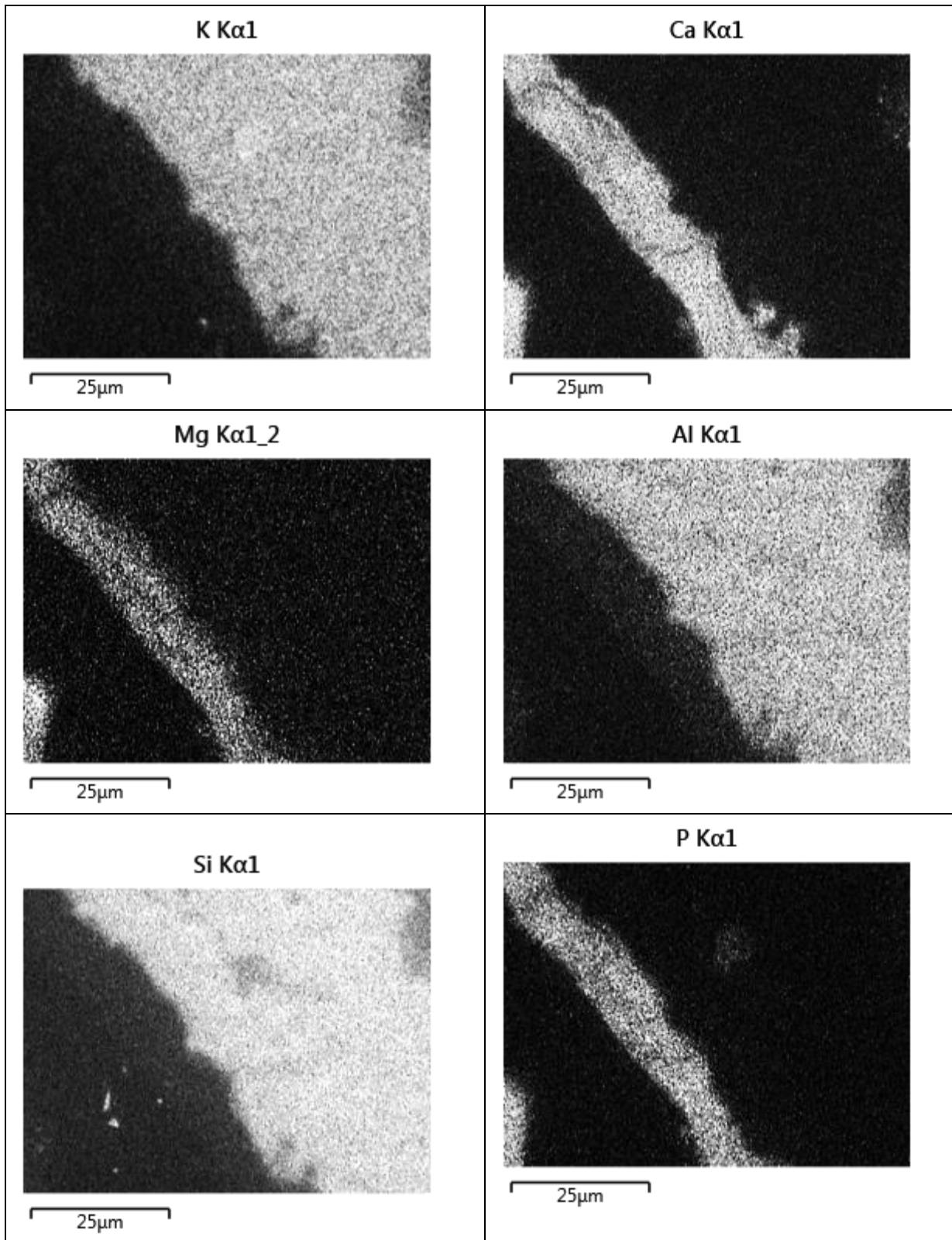


**Figure 4. Close-up of K-feldspar obtained after the combustion with bark+chicken manure.**

237 Table 4. EDS images of K-feldspar obtained after the combustion with bark+chicken manure.



238

239

240 Figure 5 shows exemplary line scans for all experiments. Line scan a) shows the developed  
 241 line after the combustion of bark. It can be seen that the concentration of Ca is increasing  
 242 towards the surface, while K is depleted. This can be seen by the deviation of the inherent K-  
 243 feldspar K/Al ratio of 1 to 0.22 in the layers formed. This substitution of K by Ca is typical for  
 244 woody biomass ash interacting with K-feldspar [8,31]. Apart from Ca and the elements  
 245 naturally contained in K-feldspar only Mg is found in a relevant amount. The line scan  
 246 measured for K-feldspar found in the sample for the gasification of bark-rich logging residues  
 247 is depicted in Figure 5 b). Similarly to the results observed for the combustion of bark, an  
 248 enrichment with Ca was detected while K is depleted. The depletion can again be  
 249 characterized by a K/Al ratio of 0.62. For this sample no Mg was observed in the layer.

250 Even though K-feldspar was only contained as an “impurity” in the olivine bed used for the  
 251 gasification of bark-rich logging residues at the CHP in Senden, the same layer formation  
 252 process took place also when no olivine was present. It is therefore possible to study the  
 253 layer formation on “impurities” and assume that the same process is occurring for a pure  
 254 bed.

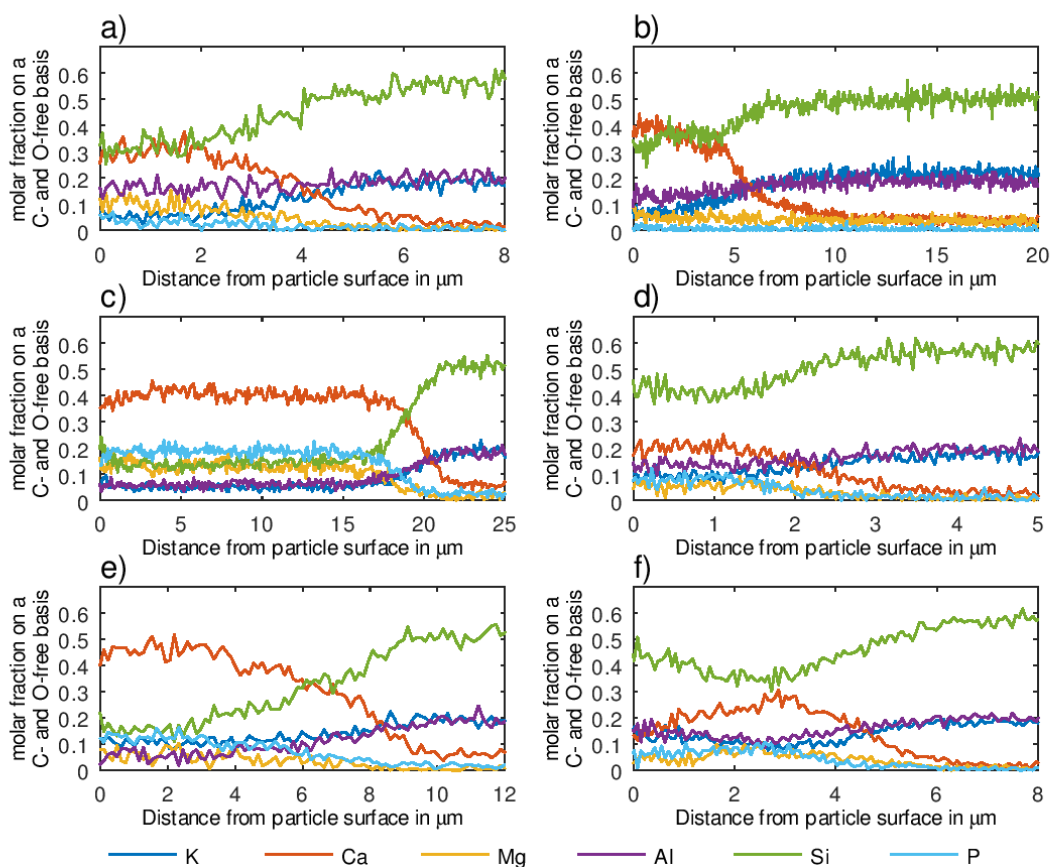


**Figure 5. Linescans measured on K-feldspar. The given distance starts at the outside of the particle and points towards the core. a) Combustion of bark b) Gasification of bark-rich logging residues c) Combustion of bark+chicken manure d) Gasification of bark+chicken manure e) Combustion of chicken manure f) Gasification of chicken manure.**

255 The layer formed during the combustion of bark+chicken manure, depicted in Figure 5 c) is  
 256 mainly dominated by Ca, P, and Mg. As already observed in Table 4 Ca seems to be found  
 257 further into K-feldspar compared to Mg and P. The same can be said for the layer formed  
 258 during the gasification of bark+chicken manure, Figure 5 d). Even though the layer is thinner,  
 259 Ca is again measured further into the particle compared to P and Mg. Apart from these three

260 elements no other elements could be found in a relevant amount. A similar observation can  
261 be made for the layers studied after the combustion and gasification of chicken manure, seen  
262 in Figure 5 e) and f), respectively. Ca is again found further into the particle, while P and Mg  
263 are enriched in the layer at the same location and no K depletion is occurring. The continued  
264 use of the bed material after the gasification of bark+chicken manure does not seem to have  
265 an influence on the formed layer during the gasification of chicken manure. This can be said,  
266 since no two separate layers different in composition were observed in the case for chicken  
267 manure, but only one layer which is similar in composition to the combustion of chicken  
268 manure. For the experiments with bark+chicken manure and pure chicken manure no  
269 depletion of K could be detected.

### 270 **3.1. Layer formation process proposal**

271 A first proposal for a possible layer formation mechanism will be given in the following  
272 section based on the data presented throughout this work. To further support the following  
273 proposal experiments focusing on long-term operation will be necessary.

274 The layers formed for bark+chicken manure and pure chicken manure are different to the  
275 layers formed with bark and bark-rich logging residue but similar to each other. For those  
276 experiments, the diffusion of K out of the K-feldspar cannot be detected. This is due to the  
277 fact that the high levels of phosphorous for bark+chicken manure and chicken manure shift  
278 the reactions into the ash phase to the formation of Ca-rich phosphates. This effect is already  
279 observable for an admixture of chicken manure of 0.3 dry mass fraction as studied here. That  
280 is due to the fact that chicken manure has a comparably high ash content, see Table 1 and  
281 Figure 3, so small admixtures already highly influence the ash chemistry. The often  
282 overlooked high Ca content of chicken manure is additionally influencing the ash chemistry.  
283 This high Ca content is promoting the formation of Ca-rich layers, which are known to be  
284 catalytically active for gasification reactions [10], also when phosphorous is present in the  
285 layers [17].

286 All line scans with bark show that Ca is penetrating further into the particle than P. This is  
287 likely due to the formation of an inner and an outer layer. If the ratio of P to Ca is further  
288 increased it was previously speculated that the inner layer might be completely inhibited.  
289 This is explained in the following. The inner layer is formed by the diffusion of Ca into the  
290 particle, while the outer layer is formed by adhesion of ash, resulting in high shares of Ca  
291 and P, which form the majority of chicken manure ash. Grimm et al. [2] have observed an  
292 inhibition of inner layer formation when using P-rich sewage sludge as feedstock and quartz  
293 particles as bed material in fluidized bed combustion experiments. The inhibition of the inner  
294 layer was explained by phosphate formation within the ash, which further leads to less  
295 reactivity of the ash components with the bed particle itself.

296 Figure 6 shows a simple scheme of inner and outer layer formation. Inner layer formation is  
297 characterized by a chemical reaction-based interaction between feedstock ash components  
298 and the bed particle surface. This interaction can be e.g. alkali-silicate formation, as  
299 observed for quartz where K reacts with silicon to form K-silicates [32]. Furthermore, inner  
300 layer formation can be based on a substitution reaction, as observed for olivine where  $\text{Ca}^{2+}$   
301 ions substitute  $\text{Fe}^{2+}$  and  $\text{Mg}^{2+}$  ions in the crystal structure of olivine. Therefore, inner layers  
302 typically grow inwards into the bed particles [33].

303 Outer layers, on the other hand, are formed through accumulation of ash components on the  
304 particle surface and pile up outwards. Woody feedstock typically shows both inner and outer

305 layer formation (Figure 6, a)), whereas P-rich residual feedstock shows a stronger tendency  
306 towards solely outer layer formation (Figure 6, b)).

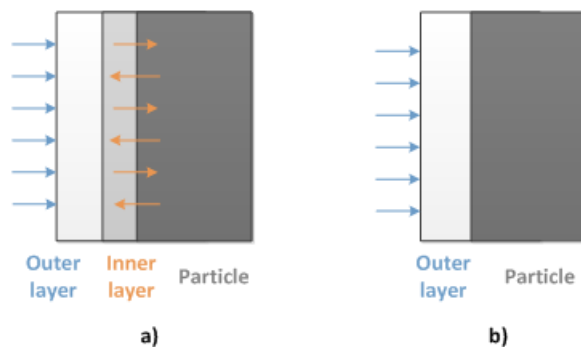


**Figure 6. Simple scheme of layer formation mechanisms; a) Chemical reaction-based layer formation with woody-based feedstock, b) Ash accumulation-based layer formation with P-rich feedstock.**

307 Frequently proposed mechanisms for layer formation in the literature [32,33] typically refer to  
308 inner layer formation since outer layers are merely an accumulation of ash components and  
309 therefore highly dependent on the feedstock ash content itself.

310 Inner layer formation has been observed to be an important factor in agglomeration in  
311 fluidized beds, as coating- or layer-induced agglomeration is a major issue when quartz  
312 particles are used as bed material [34–36]. Since outer layers are typically dominant in Ca  
313 the agglomeration tendency decreases once an outer layer – acting as a shell around the  
314 particle and, if applicable, the inner layer – has been formed. Furthermore, Ca from the outer  
315 layer can diffuse to and react with the inner e.g. K-rich layer forming a more Ca-rich inner  
316 layer with higher melting temperature. Thus, layer formation is of high relevance when it  
317 comes to investigation on agglomeration processes.

## 318 4. Conclusion

319 The presented results show that layer formation on K-feldspar is mainly dependent on the  
320 used feedstock and findings for BFB combustion and DFB gasification were similar to each  
321 other. When feedstocks rich in P are being used, an enrichment of P in the layer could be  
322 observed. Due to this it is possible to adapt the observations regarding layer formation  
323 collected for combustion to gasification applications. It was furthermore speculated that an  
324 increased P content hinders the formation of inner layers by promoting the formation of  
325 phosphates in the ash fraction. The formed phosphates then stick to the K-feldspar particles  
326 to form an ash-rich layer. This ash-rich layer forms independent of the atmosphere, i.e.  
327 combustion or gasification.

## 328 5. Acknowledgments

329 This study was carried out in the frame of the Bioenergy2020+ projects “C200410” and  
330 “N200560”. Bioenergy2020+ GmbH is funded within the Austrian COMET program, which is  
331 managed by the Austrian Research Promotion Agency (FFG) and promoted by the federal

332 government of Austria as well as the federal states of Burgenland, Niederösterreich and  
333 Steiermark.

334 Furthermore, we thank FORMAS Mobility Grant No. 2017-01613 and National Swedish  
335 Strategic Research programme Bio4Energy, Thermochemical Conversion Technologies  
336 Platform and Platform for Environment and Nutrient Recycling. We also thank the facilities  
337 and technical support (Cheng Choo Lee) of the Umeå Core Facility for Electron Microscopy  
338 (UCEM) at the Chemical Biological Centre (KBC), Umeå University.

339

340

## References

- 341 [1] W. Steffen, K. Richardson, J. Rockström, S.E. Cornell, I. Fetzer, E.M. Bennett, R.  
342 Biggs, S.R. Carpenter, W. de Vries, C.A. de Wit, C. Folke, D. Gerten, J. Heinke, G.M.  
343 Mace, L.M. Persson, V. Ramanathan, B. Reyers, S. Sörlin, Planetary boundaries:  
344 Guiding human development on a changing planet, *Science*. 347 (2015) 1259855.  
345 doi:10.1126/science.1259855.
- 346 [2] A. Grimm, N. Skoglund, D. Boström, M. Öhman, Bed Agglomeration Characteristics in  
347 Fluidized Quartz Bed Combustion of Phosphorus-Rich Biomass Fuels, *Energy Fuels*.  
348 25 (2011) 937–947. doi:10.1021/ef101451e.
- 349 [3] J.C. Schmid, U. Wolfesberger, S. Koppatz, C. Pfeifer, H. Hofbauer, Variation of  
350 feedstock in a dual fluidized bed steam gasifier—influence on product gas, tar content,  
351 and composition, *Environ. Prog. Sustain. Energy*. 31 (2012) 205–215.  
352 doi:10.1002/ep.11607.
- 353 [4] J. Karl, T. Pröll, Steam gasification of biomass in dual fluidized bed gasifiers: A review,  
354 *Renew. Sustain. Energy Rev.* 98 (2018) 64–78. doi:10.1016/j.rser.2018.09.010.
- 355 [5] D. Boström, N. Skoglund, A. Grimm, C. Boman, M. Öhman, M. Broström, R. Backman,  
356 Ash Transformation Chemistry during Combustion of Biomass, *Energy Fuels*. 26 (2012)  
357 85–93. doi:10.1021/ef201205b.
- 358 [6] H. He, D. Boström, M. Öhman, Time Dependence of Bed Particle Layer Formation in  
359 Fluidized Quartz Bed Combustion of Wood-Derived Fuels, *Energy Fuels*. 28 (2014)  
360 3841–3848. doi:10.1021/ef500386k.
- 361 [7] F. Kirnbauer, H. Hofbauer, Investigations on Bed Material Changes in a Dual Fluidized  
362 Bed Steam Gasification Plant in Güssing, Austria, *Energy Fuels*. 25 (2011) 3793–3798.  
363 doi:10.1021/ef200746c.
- 364 [8] M. Kuba, H. He, F. Kirnbauer, N. Skoglund, D. Boström, M. Öhman, H. Hofbauer,  
365 Thermal Stability of Bed Particle Layers on Naturally Occurring Minerals from Dual Fluid  
366 Bed Gasification of Woody Biomass, *Energy Fuels*. 30 (2016) 8277–8285.  
367 doi:10.1021/acs.energyfuels.6b01523.
- 368 [9] F. Kirnbauer, V. Wilk, H. Kitzler, S. Kern, H. Hofbauer, The positive effects of bed  
369 material coating on tar reduction in a dual fluidized bed gasifier, *Fuel*. 95 (2012) 553–  
370 562. doi:10.1016/j.fuel.2011.10.066.
- 371 [10] M. Kuba, F. Havlik, F. Kirnbauer, H. Hofbauer, Influence of bed material coatings on the  
372 water-gas-shift reaction and steam reforming of toluene as tar model compound of  
373 biomass gasification, *Biomass Bioenergy*. 89 (2016) 40–49.  
374 doi:10.1016/j.biombioe.2015.11.029.
- 375 [11] J. Kryca, J. Prišćák, J. Łojewska, M. Kuba, H. Hofbauer, Apparent kinetics of the water-  
376 gas-shift reaction in biomass gasification using ash-layered olivine as catalyst, *Chem.*  
377 *Eng. J.* 346 (2018) 113–119. doi:10.1016/j.cej.2018.04.032.
- 378 [12] T. Berdugo Vilches, M.C. Seemann, H. Thunman, Influence of in-bed catalysis by ash-  
379 coated olivine on tar formation in steam gasification of biomass, *Energy Fuels*. (2018).  
380 doi:10.1021/acs.energyfuels.8b02153.
- 381 [13] M. Kuba, S. Kraft, F. Kirnbauer, F. Maierhans, H. Hofbauer, Influence of controlled  
382 handling of solid inorganic materials and design changes on the product gas quality in  
383 dual fluid bed gasification of woody biomass, *Appl. Energy*. 210 (2018) 230–240.  
384 doi:10.1016/j.apenergy.2017.11.028.
- 385 [14] H. Thunman, M. Seemann, T.B. Vilches, J. Maric, D. Pallares, H. Ström, G. Berndes, P.  
386 Knutsson, A. Larsson, C. Breitholtz, O. Santos, Advanced biofuel production via  
387 gasification – lessons learned from 200 man-years of research activity with Chalmers’  
388 research gasifier and the GoBiGas demonstration plant, *Energy Sci. Eng.* 6 (2018) 6–  
389 34. doi:10.1002/ese3.188.
- 390 [15] M. Öhman, L. Pommer, A. Nordin, Bed Agglomeration Characteristics and Mechanisms  
391 during Gasification and Combustion of Biomass Fuels, *Energy Fuels*. 19 (2005) 1742–  
392 1748. doi:10.1021/ef040093w.

- 393 [16] Z. He, D.J. Lane, W.L. Saw, P.J. van Eyk, G.J. Nathan, P.J. Ashman, Ash–Bed Material  
394 Interaction during the Combustion and Steam Gasification of Australian Agricultural  
395 Residues, *Energy Fuels*. 32 (2018) 4278–4290. doi:10.1021/acs.energyfuels.7b03129.
- 396 [17] K. Wagner, A.M. Mauerhofer, M. Kuba, H. Hofbauer, Suitability of K-feldspar as  
397 Alternative Bed Material in Dual Fluidized Bed Steam Gasification in Combination with  
398 Ash-Rich Feedstocks, in: 23rd Int. Conf. FBC, Seoul, Korea, 2018: pp. 967–976.
- 399 [18] N. Berguerand, T. Berdugo Vilches, Alkali-Feldspar as a Catalyst for Biomass  
400 Gasification in a 2-MW Indirect Gasifier, *Energy Fuels*. 31 (2017) 1583–1592.  
401 doi:10.1021/acs.energyfuels.6b02312.
- 402 [19] N. Berguerand, J. Marinkovic, T. Berdugo Vilches, H. Thunman, Use of alkali-feldspar  
403 as bed material for upgrading a biomass-derived producer gas from a gasifier, *Chem.*  
404 *Eng. J.* 295 (2016) 80–91. doi:10.1016/j.cej.2016.02.060.
- 405 [20] A.M. Mauerhofer, F. Benedikt, J.C. Schmid, J. Fuchs, S. Müller, H. Hofbauer, Influence  
406 of different bed material mixtures on dual fluidized bed steam gasification, *Energy*. 157  
407 (2018) 957–968. doi:10.1016/j.energy.2018.05.158.
- 408 [21] A. Magdalena Mauerhofer, F. Benedikt, J. Christian Schmid, H. Hofbauer, Mixtures of  
409 Silica Sand and Calcite as Bed Material for Dual Fluidized Bed Steam Gasification, in:  
410 Proc. SEEP2017, University of Maribor Press, 2017: pp. 253–266. doi:10.18690/978-  
411 961-286-048-6.26.
- 412 [22] C. Pfeifer, S. Koppatz, H. Hofbauer, Catalysts for dual fluidised bed biomass  
413 gasification—an experimental study at the pilot plant scale, *Biomass Convers.*  
414 *Biorefinery*. 1 (2011) 63–74. doi:10.1007/s13399-011-0005-3.
- 415 [23] C. Pfeifer, S. Koppatz, H. Hofbauer, Steam gasification of various feedstocks at a dual  
416 fluidised bed gasifier: Impacts of operation conditions and bed materials, *Biomass*  
417 *Convers. Biorefinery*. 1 (2011) 39–53. doi:10.1007/s13399-011-0007-1.
- 418 [24] T. Berdugo Vilches, J. Marinkovic, M. Seemann, H. Thunman, Comparing Active Bed  
419 Materials in a Dual Fluidized Bed Biomass Gasifier: Olivine, Bauxite, Quartz-Sand, and  
420 Ilmenite, *Energy Fuels*. 30 (2016) 4848–4857. doi:10.1021/acs.energyfuels.6b00327.
- 421 [25] J. Marinkovic, M. Seemann, G.L. Schwebel, H. Thunman, Impact of Biomass Ash–  
422 Bauxite Bed Interactions on an Indirect Biomass Gasifier, *Energy Fuels*. 30 (2016)  
423 4044–4052. doi:10.1021/acs.energyfuels.6b00157.
- 424 [26] S. Anis, Z.A. Zainal, Tar reduction in biomass producer gas via mechanical, catalytic  
425 and thermal methods: A review, *Renew. Sustain. Energy Rev.* 15 (2011) 2355–2377.  
426 doi:10.1016/j.rser.2011.02.018.
- 427 [27] M. Kuba, F. Kirnbauer, H. Hofbauer, Influence of coated olivine on the conversion of  
428 intermediate products from decomposition of biomass tars during gasification, *Biomass*  
429 *Convers. Biorefinery*. 7 (2017) 11–21. doi:10.1007/s13399-016-0204-z.
- 430 [28] N. Skoglund, Ash chemistry and fuel design focusing on combustion of phosphorus-rich  
431 biomass, Doctoral Thesis, Department of applied physics and electronics, Umeå  
432 universitet, 2014.
- 433 [29] M. Öhman, A. Nordin, A New Method for Quantification of Fluidized Bed Agglomeration  
434 Tendencies: A Sensitivity Analysis, *Energy Fuels*. 12 (1998) 90–94.  
435 doi:10.1021/ef970049z.
- 436 [30] J.C. Schmid, Development of a novel dual fluidized bed gasification system for  
437 increased fuel flexibility, PhD Thesis, Doctoral thesis, Institute of Chemical Engineering,  
438 Vienna University of Technology, 2014.
- 439 [31] H. He, N. Skoglund, M. Öhman, Time-Dependent Layer Formation on K-Feldspar Bed  
440 Particles during Fluidized Bed Combustion of Woody Fuels, *Energy Fuels*. 31 (2017)  
441 12848–12856. doi:10.1021/acs.energyfuels.7b02386.
- 442 [32] H. He, X. Ji, D. Boström, R. Backman, M. Öhman, Mechanism of Quartz Bed Particle  
443 Layer Formation in Fluidized Bed Combustion of Wood-Derived Fuels, *Energy Fuels*. 30  
444 (2016) 2227–2232. doi:10.1021/acs.energyfuels.5b02891.
- 445 [33] M. Kuba, H. He, F. Kirnbauer, N. Skoglund, D. Boström, M. Öhman, H. Hofbauer,  
446 Mechanism of Layer Formation on Olivine Bed Particles in Industrial-Scale Dual Fluid  
447 Bed Gasification of Wood, *Energy Fuels*. 30 (2016) 7410–7418.  
448 doi:10.1021/acs.energyfuels.6b01522.



- 449 [34] H.J.M. Visser, S.C. van Lith, J.H.A. Kiel, Biomass Ash-Bed Material Interactions  
 450 Leading to Agglomeration in FBC, J. Energy Resour. Technol. 130 (2008) 011801.  
 451 doi:10.1115/1.2824247.
- 452 [35] M. Öhman, A. Nordin, B.-J. Skrifvars, R. Backman, M. Hupa, Bed Agglomeration  
 453 Characteristics during Fluidized Bed Combustion of Biomass Fuels, Energy Fuels. 14  
 454 (2000) 169–178. doi:10.1021/ef990107b.
- 455 [36] F. Scala, Particle agglomeration during fluidized bed combustion: Mechanisms, early  
 456 detection and possible countermeasures, Fuel Process. Technol. 171 (2018) 31–38.  
 457 doi:10.1016/j.fuproc.2017.11.001.

## 458 Supplementary

459 Table A.1. Fuel fingerprint data; concentrations given in mol kg<sup>-1</sup>.

	K	Na	Ca	Mg	Fe	Al	Si	P	S	Cl
Bark	0.10	0.17	0.51	0.25	0.11	0.23	0.89	0.06	0.04	0.02
Bark- rich logging residues	0.06	0.01	0.23	0.03	0.00	0.01	0.05	0.02	0.01	0.00
Bark+ chicken manure	0.24	0.23	1.11	0.45	0.10	0.22	0.81	0.60	0.13	0.12
Chicken manure	0.60	0.60	1.99	1.10	0.04	0.10	0.40	1.92	0.41	0.49

460